SNORD-host RNA *Zfas1* is a regulator of mammary development and a potential marker for breast cancer

MARJAN E. ASKARIAN-AMIRI,[1] JOANNA CRAWFORD,[1] JULIET D. FRENCH,[2] CHANEL E. SMART,[2,4]
MARTIN A. SMITH,[1] MICHAEL B. CLARK,[1] KELIN RU,[1] TIM R. MERCER,[1] ELLA R. THOMPSON,[3]
SUNIL R. LAKHANI,[4,5,6] ANA C. VARGAS,[4] IAN G. CAMPBELL,[3,7] MELISSA A. BROWN,[2] MARCEL E. DINGER,[1,8]
and JOHN S. MATTICK[1,8]

[1]Institute for Molecular Bioscience, University of Queensland, St. Lucia, QLD 4072, Australia
[2]School of Chemistry and Molecular Biosciences, University of Queensland, St. Lucia, QLD 4072, Australia
[3]VBCRC Cancer Genetics Laboratory, Peter MacCallum Cancer Centre, East Melbourne, VIC 3002, Australia
[4]The University of Queensland Centre for Clinical Research, Herston, QLD 4029, Australia
[5]School of Medicine, University of Queensland, Herston, QLD 4029, Australia
[6]Pathology Queensland, The Royal Brisbane & Women's Hospital, Herston, QLD 4029, Australia
[7]Department of Pathology, University of Melbourne, Parkville, VIC 3010, Australia

ABSTRACT

Long noncoding RNAs (lncRNAs) are increasingly recognized to play major regulatory roles in development and disease. To identify novel regulators in breast biology, we identified differentially regulated lncRNAs during mouse mammary development. Among the highest and most differentially expressed was a transcript (*Zfas1*) antisense to the 5′ end of the protein-coding gene *Znfx1*. In vivo, *Zfas1* RNA is localized within the ducts and alveoli of the mammary gland. *Zfas1* intronically hosts three previously undescribed C/D box snoRNAs (SNORDs): *Snord12*, *Snord12b*, and *Snord12c*. In contrast to the general assumption that noncoding SNORD-host transcripts function only as vehicles to generate snoRNAs, knockdown of *Zfas1* in a mammary epithelial cell line resulted in increased cellular proliferation and differentiation, while not substantially altering the levels of the SNORDs. In support of an independent function, we also found that *Zfas1* is extremely stable, with a half-life >16 h. Expression analysis of the SNORDs revealed these were expressed at different levels, likely a result of distinct structures conferring differential stability. While there is relatively low primary sequence conservation between *Zfas1* and its syntenic human ortholog *ZFAS1*, their predicted secondary structures have similar features. Like *Zfas1*, *ZFAS1* is highly expressed in the mammary gland and is down-regulated in breast tumors compared to normal tissue. We propose a functional role for *Zfas1/ ZFAS1* in the regulation of alveolar development and epithelial cell differentiation in the mammary gland, which, together with its dysregulation in human breast cancer, suggests *ZFAS1* as a putative tumor suppressor gene.

Keywords: noncoding RNA; snoRNA; tumor suppressor

INTRODUCTION

Recent high-throughput studies of gene expression have revealed there is far more genomic transcription than previously anticipated, with the majority of the genome being transcribed into non-protein coding RNAs (ncRNAs) (Kapranov et al. 2002; Carninci et al. 2005; Birney et al. 2007). Although the functional significance of various classes of small ncRNAs is becoming increasingly well-established, the functionality of the tens of thousands of long ncRNAs remains controversial (Babak et al. 2005; Brosius 2005; Struhl 2007), and their functions remain largely unknown. Large-scale studies of long ncRNAs (lncRNAs) have shown that many are dynamically regulated during differentiation and exhibit cell- and tissue-specific expression patterns (Ravasi et al. 2006; Kapranov et al. 2007a, 2007b; Mercer et al. 2008). Together with the finding that lncRNA sequences, splice sites, and promoters are subject to selection (Ponjavic et al. 2007), these observations present a compelling case that lncRNAs are generally functional. However, given the diverse nature of these transcripts, which have various genomic contexts

(intergenic, overlapping, intronic, or antisense to protein-coding mRNAs), widely different lengths (ranging from ~100 to ~100,000 bases), and may be spliced or unspliced, polyadenylated or nonpolyadenylated, and nuclear or cytoplasmically located (Dinger et al. 2009; Mercer et al. 2009), it is likely that their functions and mechanisms will also be highly diverse. Indeed, among the increasing number that have been functionally investigated (Amaral and Mattick 2008; Amaral et al. 2010), lncRNAs have been shown to function in a variety of cellular processes including transcriptional regulation (Feng et al. 2006), splicing (Yan et al. 2005), translation (Wang et al. 2005), and structure and organization of cellular components (Sunwoo et al. 2009). Furthermore, different subsets of differentially expressed ncRNAs have been identified in embryonic stem cell differentiation (Dinger et al. 2008a), T-cell differentiation (Pang et al. 2009), oligodendrogenesis (Mercer et al. 2010), and keratinocyte differentiation (Mazar et al. 2010), suggesting that any given developmental system will employ its own distinct repertoire of lncRNAs.

Although lncRNAs are difficult to classify (Mercer et al. 2009), one definable subgroup comprises host genes for small nucleolar RNAs (snoRNAs). SnoRNAs are a functionally diverse group of 60–150-nt *trans*-acting ncRNAs that function as guides for the 2′-O-ribose methylation or pseudouridinylation of ribosomal and spliceosomal RNAs. In vertebrates, most snoRNAs are intron-encoded, and their processing typically involves splicing followed by exonucleolytic trimming of the 5′ and 3′ ends. Although some snoRNA host genes encode proteins, which are primarily involved in the translational apparatus (Dieci et al. 2009), many are spliced, polyadenylated lncRNAs, which are considered to serve solely as a vehicle for snoRNA production (Pelczar and Filipowicz 1998). Structurally, snoRNAs are categorized as C/D-box snoRNAs (SNORDs) and H/ACA-box snoRNAs (SNORAs). Both SNORDs and SNORAs are dysregulated in various types of cancer and have been implicated in the development and progression of human malignancy (Dong et al. 2009; Mourtada-Maarabouni et al. 2009).

The mammary gland is one of the few organs that undergoes cycles of development and regression throughout adult life, with the full development of the gland proceeding in delineated phases: embryonic, pubertal, pregnancy, lactation, and involution (Hennighausen and Robinson 2001). Lactational development occurs with distinct morphological and molecular changes of the epithelial cells and allows for the production and secretion of milk. The secretory alveolar cells represent the final cellular state of the differentiation processes within the mammary gland (Hennighausen and Robinson 1998). These differentiation steps taking place during pregnancy and lactation are defined and characterized by the sequential activation of genes encoding the milk proteins WDNM1, β-casein, whey acidic protein (WAP) and α-lactalbumin in mouse (Robinson et al. 1995).

Further understanding the cellular pathways inherent to normal mammary growth and development is a vital precursor to elucidating the mechanisms that lead to malignant transformation in mammary epithelium. Therefore, to gain a better understanding of the molecular mechanisms that underlie development of the mammary gland and potentially breast cancer and to investigate the role of ncRNA in these processes, we performed microarray analyses and identified 97 lncRNAs that were differentially expressed in primary mammary epithelial cells of pregnant, lactating, and involuting mice.

One of the identified transcripts, *Zfas1*, exhibited an ~10-fold decrease in RNA level between pregnancy and lactation. The *Zfas1* locus is host to three C/D-box snoRNAs, and its transcription initiates from the antisense strand near the 5′ end of the protein-coding gene *Znfx1*. We determined the expression patterns of *Zfas1* and *Znfx1* during mouse mammary gland development and mammary epithelial cell differentiation. In contrast to previous assumptions that noncoding snoRNA host transcripts occurred only as vehicles to generate snoRNAs, we found that knockdown of *Zfas1* by RNA interference in a mammary epithelial cell line resulted in an increase in markers of proliferation and differentiation, despite snoRNA levels remaining relatively constant. Furthermore, we show that the three snoRNAs do not occur in equimolar ratios but rather that their relative levels can vary drastically in different conditions, suggesting their stability is tightly regulated. Given the differential expression of *Zfas1* during mammary development, we compared the expression of its human ortholog, *ZFAS1*, in a panel of matched normal and invasive ductal carcinoma tumor tissue and found *ZFAS1* is down-regulated in the tumor tissue. In summary, we propose a functional role for *Zfas1* in the regulation of the intracellular pathway affecting proliferation and milk production in the mammary gland, which, together with its dysregulation in human breast cancer, suggests *ZFAS1* as a possible tumor suppressor gene.

RESULTS

Identification of long ncRNAs that are dynamically regulated in the mouse mammary gland

To identify lncRNAs (>200 nt) involved in mammary gland development, we interrogated custom-designed microarrays with RNA extracted from primary epithelial cells isolated from mouse mammary glands at three distinct stages: 15-d pregnant, 7-d lactating, and 2-d involuting. The microarray contained probes that uniquely profile 8946 high-confidence long ncRNAs and 29,968 mRNAs (includes alternative isoforms) in mouse. Analysis of these data showed significant differential expression (B-statistic > 3; fold change > 4) of 388 mRNAs and 97 lncRNAs in developing mammary glands (Supplemental Fig. S1; Supplemental Table S1).

To validate our experimental model of the developing mammary gland, we first examined the differentially expressed coding mRNAs. The list of differentially expressed genes (Supplemental Table S1) agreed with previously reported data on mouse mammary development (Master et al. 2002) and was generally consistent with expectations of the developmental transitions under investigation (Metcalfe et al. 1999), including dynamic regulation of mRNAs with roles in cell proliferation, milk production, and apoptosis, such as Bcl2- and casein-family genes. Gene ontology (GO) analysis of differentially expressed mRNAs by Babelomics (Al-Shahrour et al. 2006) showed enrichment in genes associated with regulation of cell growth and size and response to hormone stimulus (Supplemental Fig. S2). Based on these observations, we anticipated that the differentially expressed lncRNAs should be similarly relevant to the biological processes underlying mammary development. Indeed, among the differentially expressed lncRNAs, we identified known lncRNAs, such as Dio3os, which has previously been associated with decreased proliferation and increased differentiation of precursor cells to mature adipocytes, analogous to the transition from pregnancy to lactation during mammary gland development (Hernandez et al. 2007).

Zfas1 is a highly expressed, spliced lncRNA that is regulated during mammary gland development

To identify lncRNAs for subsequent experimental examination, we ranked the list of significantly differentially expressed lncRNAs by fold change and absolute expression level. Next, on the basis that many lncRNAs originate from complex transcriptional loci (Engstrom et al. 2006) in which they may have a functional relationship with the nearby protein-coding genes, we further refined our list of lncRNAs by examining their genomic context. Using our previously described classifications of lncRNA loci (Dinger et al. 2009), we identified 15 cis-antisense, 3 nearby antisense, 37 intronic, and 42 intergenic transcripts (Supplemental Table S1). Because we were interested in lncRNAs that may impact on human mammary development, we further refined our list of candidates by considering only those for which there was transcriptional evidence at the syntenic genomic position in human. In total, 19 of the 97 transcripts had human transcripts that arose from syntenic locations.

Taken together, our criteria highlighted a previously uncharacterized lncRNA, which had been annotated in RefSeq as 1500012F01Rik (GenBank ID AK005231). Transcription of this spliced lncRNA initiates from the nearby antisense strand of the Znfx1 (zinc finger NFX-1-type containing) promoter region (Fig. 1A; Supplemental Fig. S3), which led to our naming of it as Zfas1 (zinc finger antisense). As Zfas1 is not transcribed from an ultra-conserved region (Bejerano et al. 2004) and is located close

to a protein-coding gene, it does not belong to the existing lncRNA subclasses of T-UCRs (transcribed ultraconserved RNAs) (Calin et al. 2007) or lincRNAs (long intergenic noncoding RNAs) (Guttman et al. 2009). From our list of differentially expressed lncRNAs, Zfas1 was the second most highly expressed (A-value ~10) and had the second largest fold change (34-fold down-regulated from pregnant to lactating) (Supplemental Table S1; Supplemental Fig. S4). In human, the ZNFX1 locus also features an equivalently positioned spliced noncoding transcript, which is annotated in RefSeq Genes as NCRNA00275, a feature not shared by the other highly differentially expressed transcripts. Another interesting feature of this transcript is that it hosts three snoRNA genes, Snord12, Snord12b, and Snord12c, within sequential introns (Fig. 1A; Supplemental Fig. S3; Supplemental Table S2). The combination of these characteristics led us to pursue Zfas1 for further characterization in mammary development.

Although our ncRNA annotation program had indicated that Zfas1 was noncoding, we noted that the sequence did contain a 79-amino acid open reading frame (ORF). Using BLASTP, we confirmed that this protein sequence was not conserved among mammals and did not contain any known protein motif. Moreover, the start and stop codons were not conserved in the human ortholog of Zfas1, and there was no evidence of any consensus ribosomal binding sequences. Analysis by the CRITICA algorithm (Badger and Olsen 1999) also indicated that the codon usage frequency of this ORF was inconsistent with other mouse genes. Querying PRIDE, a database of peptide sequences deduced from proteomic analyses (Vizcaino et al. 2009), showed no peptides have been identified that correspond to the Zfas1 ORF. Together, these observations led us to conclude that the transcript was unlikely to encode a protein.

Zfas1 expression is differentially regulated to Znfx1

As shown in Figure 1A, Zfas1 and Znfx1 are closely positioned in a head-to-head orientation and potentially share a bidirectional promoter. This raises the possibility that these genes may be coordinately regulated (Trinklein et al. 2004; Engstrom et al. 2006; Dinger et al. 2008a; Mercer et al. 2008). To investigate whether Zfas1 and Znfx1 are coregulated, we examined their expression profiles at different stages of mammary gland development by quantitative real time PCR (qPCR). Figure 1B illustrates the expression of these two genes relative to Tubulin delta 1 (Tubd1), a result in agreement with the microarray data (Supplemental Fig. S4). Although Zfas1 was significantly down-regulated (ninefold) between pregnancy and lactation and significantly up-regulated between lactation and involution (fourfold), Znfx1 did not change appreciably during these transitions. This, together with the finding that the ratio of Zfas1 to Znfx1 varies from 63:1 (in pregnancy) to 6:1 (in lactation) in different developmental
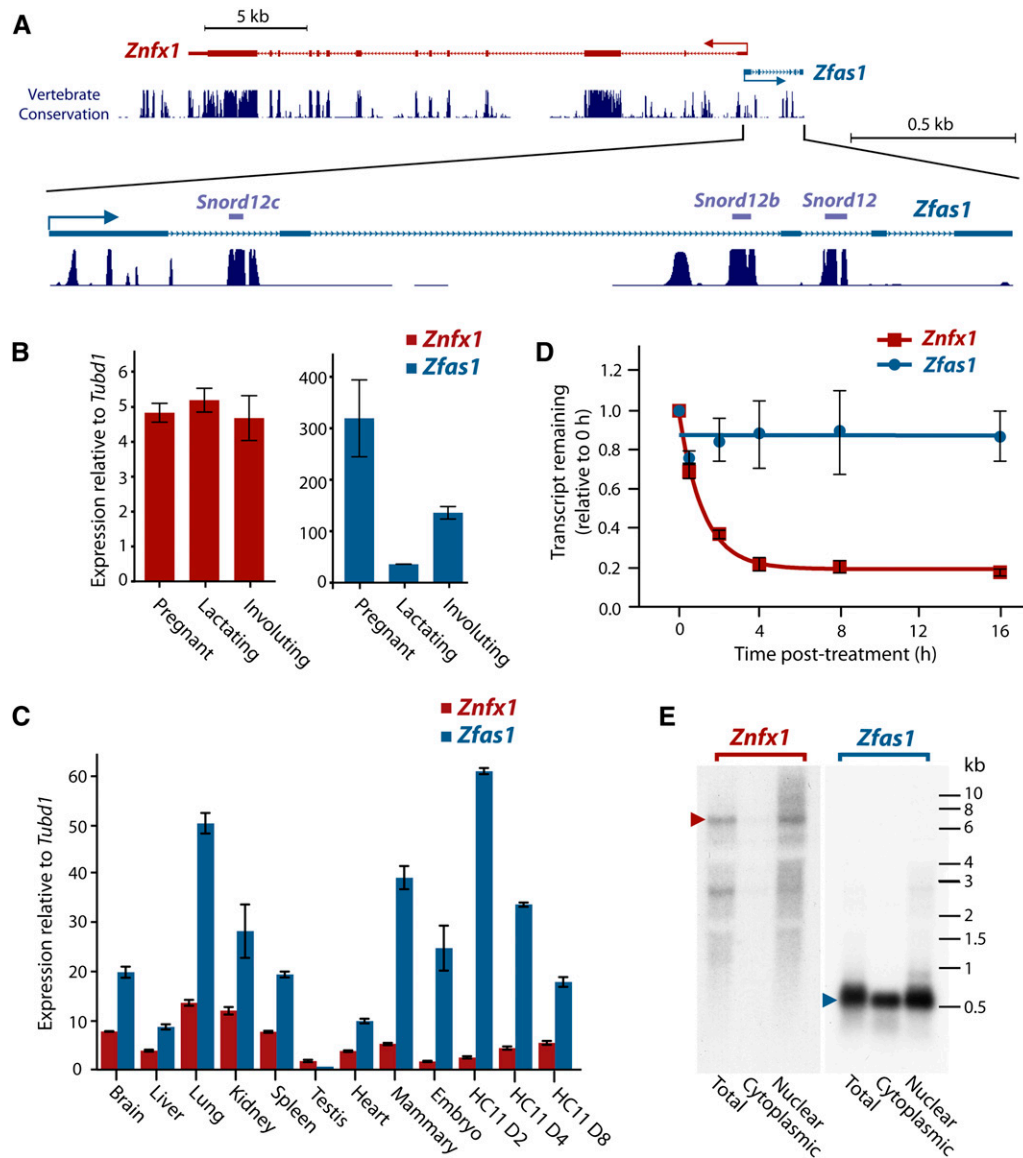
FIGURE 1. Relationship and expression of *Znfx1* and its associated ncRNA *Zfas1*. (*A*) Genomic context of *Znfx1* and its associated ncRNA. The enlarged *Zfas1* indicates the location of three snoRNAs derived from this gene. The high degree of conservation of these regions across mammalian species is indicated. (*B*) Relative expression of *Znfx1* (*left*) and *Zfas1* (*right*) in mammary epithelial cells during different developmental stages of mammary gland development to Tubulin delta 1 (*Tubd1*). Expression levels of three biological replicates for each stage were measured in triplicate by qPCR. (*C*) Relative expression profile of *Znfx1* and *Zfas1* to *Tubd1* in different tissues by qPCR. Technical replicates were performed in triplicate for each sample. (*D*) Decay curve of *Znfx1* and *Zfas1* in N2A cells. Transcription was blocked by treatment with actinomycin D, and expression levels of three biological replicates were detected by qPCR. Error bars in *B*, *C*, and *D* are the standard error of the mean (SEM). (*E*) Northern blot analysis of *Znfx1* and *Zfas1* on RNA derived from total, cytoplasmic, and nuclear fractions of HC11 cells. Arrows indicate size of transcript for each gene.

stages of the mammary gland, suggests that the transcripts are independently regulated.

EST evidence from GenBank showed that *Znfx1* and *Zfas1* were expressed in many other tissues outside of the mammary gland, including kidney, brain, pancreatic bud, thymus, eye, heart, and embryo. To obtain a more comprehensive profile of the relative expression levels of *Znfx1* and *Zfas1* in mouse, we performed qPCR on a diverse range of tissues. Figure 1C shows the expression of *Znfx1* is

significantly lower than *Zfas1* in each of the tissues examined (except testis). Although the expression profiles of *Zfas1* and *Znfx1* were positively correlated (Pearson co-efficient, $R = 0.77$), the ratios of *Zfas1* to *Znfx1* varied considerably, ranging from 1:2.6 in testis to 7.4:1 in mammary gland (Supplemental Fig. S5). The data shows that the highest level of expression of *Zfas1* occurs in the lung followed by mammary gland and, in contrast, is almost undetectable in testis. Interestingly, the lung and

mammary gland both have biologically similar alveolar structures, raising the possibility that *Zfas1* may play a role in alveolar morphogenesis.

In addition to the various tissues, we also examined the relative expression of *Zfas1* and *Znfx1* in the murine mammary epithelial cell line HC11 during an 8-d in vitro assay. After an initial proliferative phase in the presence of epidermal growth factor (day 2), addition of lactogenic hormones to the HC11 cells at day 4 stimulates lactogenic differentiation in the formation of dome-like structures and the expression of milk proteins by day 8. As well as again showing discordant expression between *Zfas1* and *Znfx1*, the results show that *Zfas1* is both highly expressed in HC11 cells and is down-regulated upon differentiation (Fig. 1C; Supplemental Fig. S5). This is consistent with our observation of the differential expression of *Zfas1* in the mammary gland and suggests that HC11 cells serve as a meaningful experimental model to explore *Zfas1* function.

Given the overlapping promoter regions of *Znfx1* and *Zfas1*, the highly discordant expression of these transcripts is surprising. One explanation for this observation is that *Zfas1* is more stable than *Znfx1*, resulting in higher steady-state levels. To examine this hypothesis, we treated N2A cells with the general transcription inhibitor actinomycin D and quantified the expression levels after 0.5, 2, 4, 8, and 16 h (Fig. 1D). We calculated that *Znfx1* had a mean half-life of 50 min (95% confidence interval; 41–65 min). In contrast, *Zfas1* levels did not decline significantly after 16 h (relative to GAPDH), confirming that this transcript is indeed highly stable.

As a number of previously characterized lncRNAs have been shown to act in the nucleus (Wilusz et al. 2009), we performed Northern blot analysis on total, nuclear, and cytoplasmic RNA derived from HC11 cells using probes targeting *Zfas1* and *Znfx1* (Fig. 1E). The Northern hybridization for *Zfas1* identified a single strong band of 0.5 kb, which is consistent with the length of the full-length cDNA clones of *Zfas1*. The Northern hybridizations revealed that *Zfas1* was expressed in both cytoplasmic and nuclear fractions, while *Znfx1* was highly enriched in the nucleus.

Zfas1 is expressed in the epithelial cells of the duct and alveoli of the mammary gland

To further analyze *Zfas1* expression, we performed section in situ hybridization (ISH) on mammary glands dissected from 15-d pregnant mice. DIG-labeled

in vitro transcribed *Zfas1* RNA was used to detect expression in section paraffin-embedded pregnant mammary gland. The staining revealed enrichment of *Zfas1* expression in the epithelial cells of the ducts and alveoli of the pregnant mammary gland (Fig. 2) relative to the background. Together with the high expression of *Zfas1* observed in mammary gland and lung generally, this result is consistent with the notion that *Zfas1* is involved in alveolar development.

Knockdown of *Zfas1* results in an increase in markers of cell proliferation

In light of the observation that *Zfas1* expression was increased in the mammary gland during pregnancy when the cells are most proliferative, we hypothesized that *Zfas1* may have a role in cell proliferation. To investigate the effect of *Zfas1* on cell proliferation, we knocked down its expression in exponentially growing HC11 cells using several small interfering RNAs (siRNAs) specific to *Zfas1*. Using qPCR to measure the relative expression levels of *Zfas1*, we observed a reduction in expression of *Zfas1* relative to a scrambled siRNA-transfected control of at least 80%, which was maintained for up to 4 d in the *Zfas1*-specific siRNA-treated cells (Fig. 3A; Supplemental Fig. S6). We also assayed *Znfx1* expression to see if attenuation of *Zfas1* expression had an effect on its protein-coding partner. As seen in Figure 3A, a similar but slightly offset change in expression was apparent for *Znfx1* over the same period of analysis.
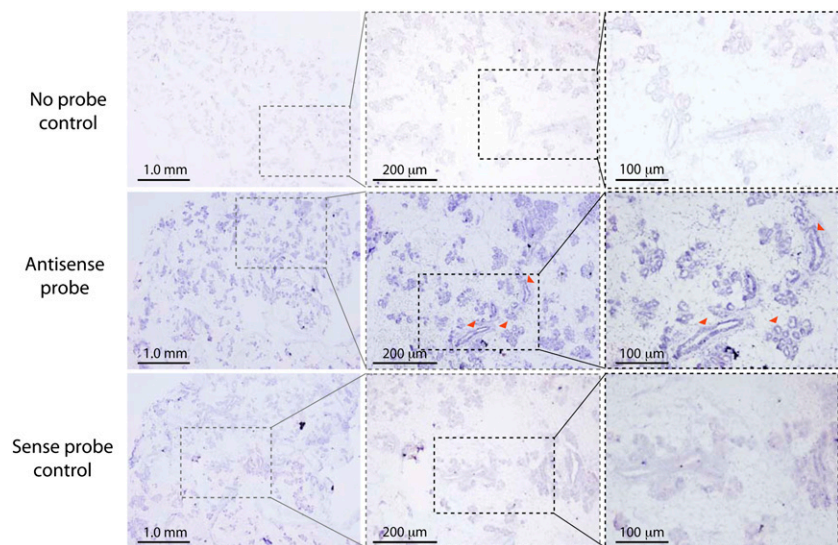
FIGURE 2. ISH mammary gland sections from pregnant mice. Panels illustrate mammary gland sections hybridized with no probe (*top*; negative control), *Zfas1* antisense probe (*middle*), and *Zfas1* sense probe (*bottom*; negative control). Images in dotted boxed areas increase in magnification from *left* to *right*. The arrows show ductal and alveolar structure and the expression of *Zfas1* within these structures. Scale bars in each panel are indicated. The genomic context of the ISH probe is shown in Supplemental Fig. S3.
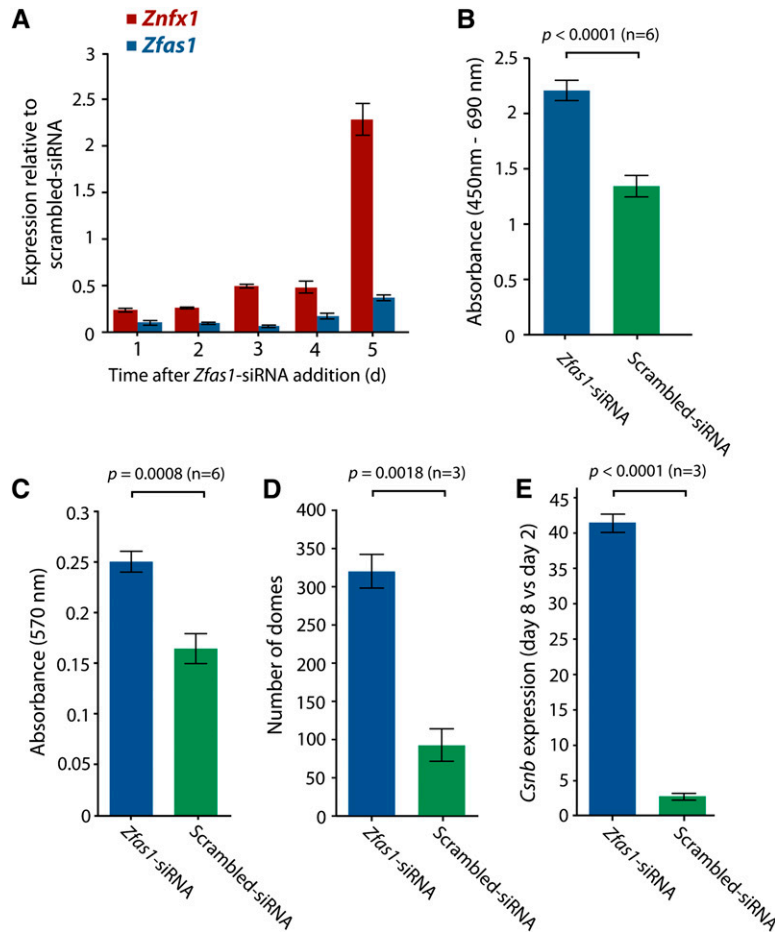
FIGURE 3. Effect of *Zfas1* knockdown by RNA interference. (*A*) The expression level, normalized to *Tubd1*, of *Znfx1* and *Zfas1* genes in HC11 cells transfected with *Zfas1* siRNA relative to the respective expression of each gene in HC11 cells transfected with scrambled siRNA measured by qPCR 1–5 d after siRNA transfection. Technical replicates were performed in triplicate for each time point, with error bars indicating SEM. (*B*) Proliferation rates based on level of BrdU incorporation measured 48 h after cells were transfected with *Zfas1* versus scrambled siRNA. Six technical replicates were performed with error bars indicating SEM. (*C*) MTT assay measuring the metabolic rate of HC11 cells transfected with *Zfas1* versus scrambled siRNA. Six technical replicates were performed with error bars indicating SEM. (*D*) Effect of *Zfas1* knockdown compared to the scrambled siRNA control on dome formation in differentiated HC11 cells measured on day 8. (*E*) Quantitative PCR, relative to *Tubd1*, of β-casein (*Csn2*) levels in differentiated (day 8) cells relative to undifferentiated (day 2) in HC11 cells transfected with *Zfas1* or scrambled siRNA. The results in *D* and *E* represent data from three experiments, each with three technical replicates, with error bars indicating the SEM of the three experiments.

Cell proliferation rates were determined by quantifying incorporation of BrdU into DNA 48 h after cells were transfected by siRNA (Fig. 3B). We found that the *Zfas1*-knockdown cells displayed a higher rate of proliferation relative to the scrambled siRNA-transfected control. To further validate this effect, we also measured proliferation rates in *Zfas1* knockdown and control cells using an MTT [3-(4,5-dimethylthiazol-2-yl)-2,5-diphenyltetrazolium bromide, a tetrazol] assay (Mosmann 1983) to measure metabolic activity over a 4-h period. Consistent with the BrdU incorporation assay, cells transfected with siRNAs targeting

Zfas1 showed increased proliferation (Fig. 3C). Together, these results suggest that *Zfas1* may play a role in regulating cell proliferation.

Knockdown of *Zfas1* induces β-casein expression and epithelial dome formation

To explore the hypothesis that *Zfas1* has a regulatory role in alveolar development in the mammary gland, we examined the effect of knocking down *Zfas1* during a dome formation assay. Formation of domes in cell culture, which can be induced in HC11 cells by addition of o-prolactin and dexamethasone, is considered to be a model for mammary epithelial cell differentiation (Zucchi et al. 2002). Relative to a scrambled siRNA control, HC11 cells that had been transfected with a *Zfas1*-targeted siRNA showed a marked increase in the number of domes formed following induction (Fig. 3D). O-prolactin- and dexamethasone-induced HC11 differentiation is also characterized by increased expression of β-casein. To further characterize the role of *Zfas1* in this developmental model, we determined the response to *Zfas1*-knockdown in comparison to a scrambled siRNA-knockdown by measuring the expression level of *Csn2* (β-casein) in differentiated (day 8) relative to undifferentiated (day 2) cells. We found that in *Zfas1* knockdown cells, the expression of *Csn2* increased over 40-fold in differentiated cells relative to undifferentiated cells, whereas it increased just twofold in cells transfected with the control siRNA (Fig. 3E). Together, these results suggest that *Zfas1* may play a role in regulating HC11 differentiation.

SnoRNAs derived from *Zfas1* are differentially expressed

Zfas1 is predicted to host three C/D box-containing homologous snoRNA genes, *Snord12*, *Snord12b*, and *Snord12c*, in consecutive introns (Fig. 1A). Intronic snoRNAs have been identified in all eukaryotic genomes and are frequently distributed in noncoding genes in this manner, with one snoRNA per consecutive intron (Huang et al. 2005). C/D box snoRNAs primarily guide the site-specific methylation of other RNAs, mainly ribosomal RNAs. *Snord12* and

Snord12b (previously referred to as MBII-99 and MBII-99B) are predicted to modify Gm3868 and Gm3878, respectively, in 28S rRNA (Huttenhofer et al. 2001; Yang et al. 2006). *Snord12c* (previously referred to as *Snord106* or *U106*) contains antisense elements that match the G1536 and U1602 segments in 18S rRNA. However, as there is no evidence for methylation at these sites, *Snord12c* may function solely as an RNA chaperone or target chemical modifications in a nonribosomal transcript. The predicted size for *Snord12*, *Snord12b*, and *Snord12c* are ∼85, ∼87, and ∼93 nucleotides, respectively.

As the three *Zfas1* snoRNAs had not previously been examined in mouse (*Snord12b* and *Snord12c* are unannotated in RefSeq and UCSC Known Genes), we designed primers to detect the expression of these SNORDs. Using cDNA prepared from mouse mammary epithelial cells, we were able to confirm the existence of all three snoRNAs. Next, we aimed to determine the relative expression levels of *Snord12*, *Snord12b*, and *Snord12c* in mammary epithelial tissue from pregnant, lactating, and involuting mice. Using

qPCR (TaqMan), each of the snoRNAs was found to be most highly expressed during pregnancy (Fig. 4A), consistent with the higher expression of the host transcript *Zfas1* in pregnancy. However, in contrast to *Zfas1*, which shows increased expression in involuting relative to lactating mammary epithelial cells, the SNORDs are expressed at similar levels at these developmental stages. Surprisingly, given that the three snoRNAs are derived from the same host transcript, *Snord12b* was expressed at up to 171-fold and 72-fold greater levels than *Snord12c* and *Snord12*, respectively. To examine whether the expression trends of *Snord12*, *Snord12b*, and *Snord12c* were similar in differentiating HC11 cells, we used qPCR to examine their expression levels in 2-, 4-, and 8-d differentiated HC11 cells (Fig. 4B). Although we found *Snord12b* was more highly expressed than *Snord12* and *Snord12c*, the difference in expression was much less dramatic (approximately eight-fold and approximately fivefold for *Snord12c* and *Snord12*, respectively). Similar to the expression trend of *Zfas1*, the snoRNAs were consistently most highly expressed in
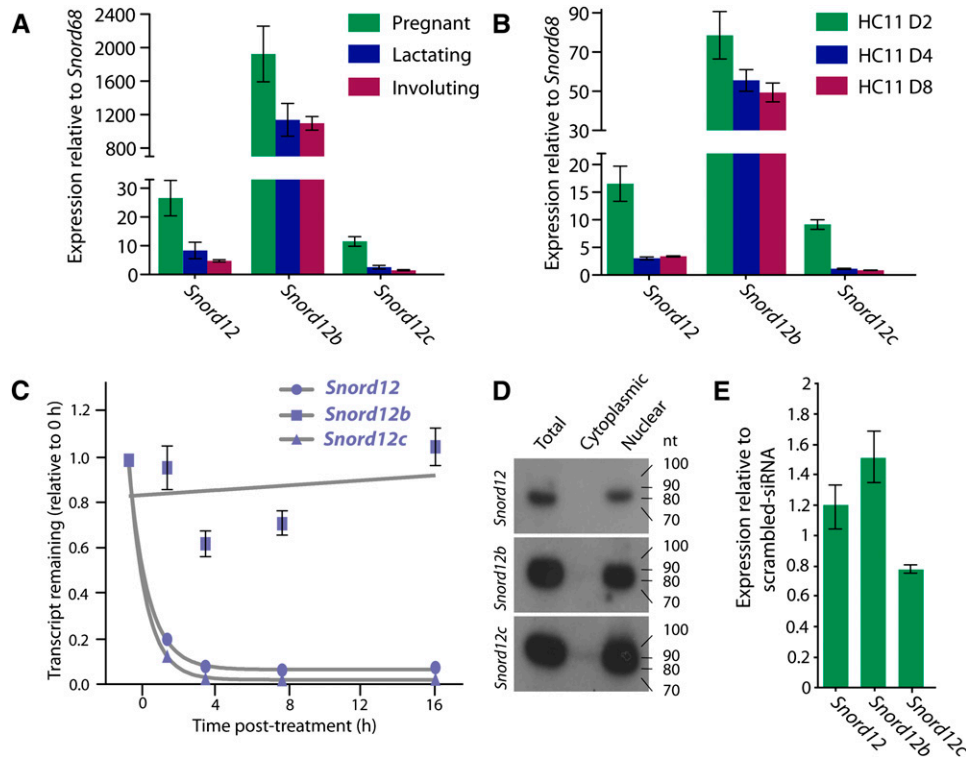
FIGURE 4. Expression of snoRNAs that are intronic to *Zfas1*. (*A*) Relative expression (from *left* to *right*) of *Snord12*, *Snord12b*, and *Snord12c* to *Snord68* during different mammary gland developmental stages. Expression levels of three biological replicates for each stage were measured in triplicate by qPCR. (*B*) Expression levels (from *left* to *right*) of *Snord12*, *Snord12b*, and *Snord12c* during HC11 cell differentiation relative to *Snord68*. Expression levels of two biological replicates for each stage were measured in triplicate by qPCR. Error bars in both *A* and *B* are SEM of the biological replicates. (*C*) Decay curve of *Snord12*, *Snord12b*, and *Snord12c* in N2A cells. Transcription was blocked by treatment with actinomycin D, and expression levels were detected in triplicate by qPCR. Errors are the standard error of the mean (SEM). (*D*) Northern blot analysis of *Snord12*, *Snord12b*, and *Snord12c* (see Fig. 1A and Supplemental Fig. S3 for genomic positions) expression in total, cytoplasmic, and nuclear RNA derived from undifferentiated HC11 cells. (*E*) Expression levels of *Snord12*, *Snord12b*, and *Snord12c*, normalized to *Snord68*, in undifferentiated (day 2) HC11 cells transfected with *Zfas1* siRNA relative to expression levels of each normalized gene in HC11 cells transfected with scrambled siRNA. Technical replicates were performed in triplicate, with error bars indicating SEM.

undifferentiated HC11 cells (day 2) and decreased significantly in differentiated (day 4 and 8) cells.

One explanation for the highly differential molar ratios of *Snord12*, *Snord12b*, and *Snord12c* is that they have different stabilities. Using the same approach as described above to determine the stability of *Znfx1* and *Zfas1*, we blocked transcription and determined the expression levels of the three SNORDs. We found that *Snord12* and *Snord12c* levels decreased rapidly (with half-lives of 43 min and 37 min, respectively) following transcriptional inhibition, whereas *Snord12b* levels did not change appreciably even after 16 h (Fig. 4C). Although these snoRNAs are similar in sequenc and are accordingly considered to belong to the same family, we hypothesized that they may fold into different structures. To examine this hypothesis, we used MFOLD to predict the secondary structures of the three snoRNAs (see Supplementary Methods). Interestingly, *Snord12b*, which had exhibited much higher expression levels than *Snord12* and *Snord12c*, folded into a distinct structure with an additional short hairpin in relation to *Snord12* and *Snord12c*, which folded into the traditional secondary structure of C/D box snoRNAs (Supplemental Fig. S3).

As the *Zfas1* transcript was detected in both nuclear and cytoplasmic fractions of HC11 cells, we examined the cellular localization of the snoRNAs. We prepared total RNA from HC11 cells and subsequently fractionated the cells into nuclear and cytoplasmic portions. Consistent with the qPCR data, Northern blot analysis indicated a high level of expression for all three *Zfas1*-derived snoRNAs, but unlike *Zfas1*, SNORD expression was specific to the nuclear fraction of these cells (Fig. 4D). The Northern analysis showed a single band of the predicted size for each snoRNA. The absence of smaller fragments in the Northern blot as well as examination of small RNA deep sequencing data (Taft et al. 2009) suggests that, unlike previous reports of other snoRNAs (Ender et al. 2008; Taft et al. 2009), *Snord12*, *Snord12b*, and *Snord12c* are not processed into smaller RNAs.

Although the siRNA-mediated knockdown of *Zfas1* should not affect the expression of *Snord12*, *Snord12b*, and *Snord12c*, which we would expect to be spliced out of the *Zfas1* prior to siRNA-directed breakdown of the host transcript, we nevertheless wished to confirm that the phenotypic changes observed during *Zfas1*-knockdown were not a direct consequence of reduced SNORD expression. Using qPCR, we found that there are only minor differences in the expression of *Snord12, Snord12b,* and *Snord12c* in the *Zfas1*-knockdown compared to the scrambled siRNA control (Fig. 4E). These small changes in expression, relative to the ∼80% knockdown of the host transcript, suggest that the phenotypic changes observed following *Zfas1* knockdown are a consequence of the host transcript and that the mature form of *Zfas1* functions intrinsically as an RNA.

Human *ZFAS1* transcript exists and undergoes regulated alternative splicing

The human ortholog of *Zfas1*, *ZFAS1*, is located on chromosome 20. In terms of the relative position of its transcription start site to *ZNFX1* and the presence of intronic snoRNA genes (Fig. 5A), the *ZFAS1* locus is similar to that in mouse. *ZFAS1* is alternatively spliced with cDNA evidence indicating the presence of at least five different isoforms. Although the snoRNA genes (*SNORD12*, *SNORD12B*, and *SNORD12C*) are highly conserved between mouse and human (81.3%, 68.9%, and 71%, respectively), a comparison of the exonic regions of the most prevalent isoforms of *ZFAS1* (isoforms 1-4 in Figure 5A; *C20orf1999* uc002xuj.2, uc002xul.3, uc002xum.3, uc002xuo.2) with its mouse ortholog (NM_001081005.1) shows an average of only 43% identity. However, comparison of the secondary structure predictions of the mature *Zfas1* and *ZFAS1* transcripts revealed several highly structured regions of the transcripts were very similar despite lacking sequence identity (Supplemental Fig. S7).

To obtain an overview of *ZNFX1* and *ZFAS1* expression, we performed qPCR across a panel of 20 human tissues and the breast cancer cell lines MCF7, BT474, and T47D (Supplemental Figs. S8, S9). Similar to the mouse tissue data, the ratios of *ZFAS1* to *ZNFX1* varied across tissues (from 2:1 in testis to 12:1 in mammary tissue). However, overall there was a positive correlation (Pearson's correlation, $R^2 = 0.797$, $n = 20$) between the expression profiles of *ZNFX1* and *ZFAS1* across the tissue samples (Supplemental Fig. S8). Analysis of publicly available transcriptomic deep sequencing data in normal human breast tissue and mammary epithelium (Wang et al. 2008) mirrored our expression analysis in mouse, showing that *ZFAS1* is very highly expressed in mammary tissue (in the top 2%–5% of all genes) (Fig. 5B).

The deep sequencing data recapitulated the presence of at least three different isoforms of *ZFAS1*. Furthermore we were able to detect *ZFAS1* isoforms in RNA isolated from MCF7, BT474, and T47D by using PCR primers designed to common exons (Supplemental Fig. S9). To determine whether different isoforms were alternatively regulated in different tissue types, we examined the relative proportions of the isoforms in the RNA deep sequencing libraries. Although the longer isoforms were predominant in each tissue type (ranging from ∼55% to ∼85% of the three distinguishable groups), the relative proportions of the isoform groups differed between tissue types, suggesting regulation of the alternative splicing (Fig. 5C; Supplemental Fig. S9).

Human *ZFAS1* levels are reduced in ductal carcinoma relative to normal breast tissue

Given the role of *Zfas1* in proliferation, we hypothesized that decreased *ZFAS1* expression may be a marker for
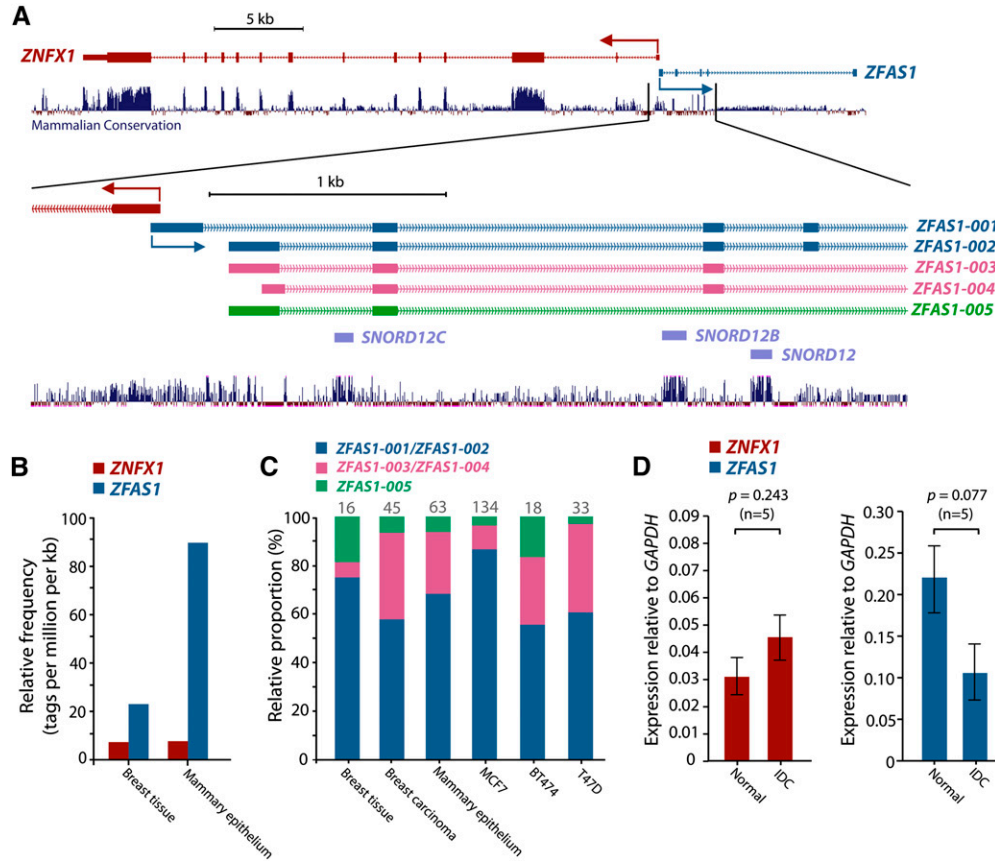
FIGURE 5. Expression analysis of human *ZFAS1*. (*A*) Genomic context of human *ZNFX1* and *ZFAS1*. The 5′ ends of *ZNFX1* and *ZFAS1* are oriented head-to-head on opposite strands. The zoomed-in regions show five different *ZFAS1* isoforms that are represented by ESTs. The positions of the intronically-derived snoRNAs—*SNORD12*, *SNORD12B*, and *SNORD12C*—are also shown with the degree of conservation across mammalian species indicated. (*B*) Comparative expression levels (tpm) of *ZNFX1* and *ZFAS1* based on RNA deep sequencing of human breast tissue and mammary epithelium. (*C*) Relative abundance of alternate isoforms of *ZFAS1* in various human tissues and cell lines based on exon-exon junction spanning deep sequence tags. The number on *top* of each bar represents the number of informative tags. (*D*) Relative expression level of *ZNFX1* and *ZFAS1* to *GAPDH* in the five paired normal and invasive ductal carcinoma (IDC) samples detected by qPCR with technical replicates performed in triplicate. Error bars indicate SEM of the biological replicates.

breast cancer and, moreover, that *ZFAS1* may be a tumor suppressor gene. To investigate this hypothesis, we examined *ZFAS1* expression in total RNA isolated from the epithelial cells isolated by micro-dissection from frozen sections of normal breast and invasive ductal carcinoma (IDC) tissue (five paired and seven unpaired samples). The result shows *ZFAS1* expression is decreased (2.0-fold, $p = 0.08$, paired; 2.7-fold, $p = 0.09$, unpaired) in ductal carcinoma relative to normal epithelial cells (Fig. 5D; Supplemental Fig. S10). Taken together with the effects of *Zfas1* knockdown on mammary epithelial cell proliferation and differentiation, our results suggest *ZFAS1* as a novel human tumor suppressor gene in breast cancer and that its dysregulation may be useful as a marker for breast cancer.

DISCUSSION

Although the importance of lncRNAs in cell function is now becoming firmly established (Mercer et al. 2009), only

a relatively small number have been shown to be involved in cancer (Huarte and Rinn 2010). In light of the potential value of lncRNAs as biomarkers and therapeutic targets (Huarte and Rinn 2010), as well as to further our understanding of the molecular mechanisms underlying cancer formation and development, we sought to identify lncRNAs involved in breast cancer. Under the hypothesis that lncRNAs involved in mammary development may be dysregulated in breast cancer, we examined the expression of 8946 lncRNAs at different stages of mouse mammary gland development and found a total of 97 that showed significant dynamic changes. We ranked the candidates on the basis of overall expression level, fold change, and conservation in humans. As a result, we selected the lncRNA *Zfas1*, which is positioned on the antisense strand at the 5′ end of the *Znfx1* protein-coding gene and is host to three C/D box snoRNAs, for further functional examination.

Knockdown of *Zfas1* in mouse mammary epithelial cells resulted in a significant increase in proliferation and

metabolic activity. Examination of the expression of the intronically hosted SNORDs following knockdown showed that their expression was only minimally altered, suggesting that the processed *Zfas1* transcript is itself functional. The high level of proliferation and low level of *Zfas1* expression is analogous to our observations in human mammary tissues, where we observe a substantially decreased level of *ZFAS1* in highly proliferative invasive ductal carcinoma cells compared to normal breast tissue. Collectively, these observations led us to propose *ZFAS1* as a putative tumor suppressor gene.

The head to head arrangement between *Zfas1* and the oppositely transcribed protein-coding gene *Znfx1* occurs frequently in mammalian genomes (Trinklein et al. 2004; Engstrom et al. 2006). *Znfx1* and *Zfas1* share a CpG island, the methylation of which would be expected to similarly affect the expression of these transcripts. Although in some cases such bidirectional genes show concordant expression profiles, consistent with the notion of shared regulatory elements, others, as described below for *Znfx1* and *Zfas1*, share more complex expression relationships (Dinger et al. 2008a; Mercer et al. 2008). In both mouse and human, the expression patterns of *Znfx1* and *Zfas1* were similar over a panel of tissues, with the exception of testis and mammary gland. In both species, relative to *Znfx1*, *Zfas1* was considerably down-regulated in testis and up-regulated in mammary gland. The uncoupling of *Znfx1* and *Zfas1* expression was also evident both in the developing mammary gland, where *Znfx1* remains relatively constant while *Zfas1* undergoes significant dynamic changes, and during differentiation of the mouse mammary epithelial cell line HC11, where there was an inverse relationship in the expression of *Zfas1* and *Znfx1*. Furthermore, knockdown of *Zfas1* in HC11 cells results in a concomitant relative decrease in *Znfx1* expression levels. However, as the levels of *Zfas1* recovered following knockdown, there was an overcompensation of *Znfx1*, which increased to more than twofold that of normal cells. Together, these observations suggest that the expression of *Znfx1* and *Zfas1* is likely to be intertwined and therefore may participate in the same regulatory network. However, because the expression of these genes can be uncoupled in some conditions, it is likely that there are at least some independent regulatory controls underlying their expression and/or stability. Furthermore, the specific up-regulation of *Zfas1* relative to *Znfx1* in mammary gland suggests a specific role for *Zfas1* in this organ, particularly during development.

Although the Znfx1 protein has not been previously studied, its predicted sequence contains an NFX-1 (nuclear transcription factor X-box binding) zinc finger domain. Despite the low homology between the NFX-1 binding domain and the corresponding region in Znfx1, (26% identity; 36% similarity over a 327-amino acids region), the critical cysteine residues that characterize the domain (Song et al. 1994) are highly conserved (36/40; 90%),

suggesting that Znfx1 may also bind DNA. Interestingly, the human ortholog of *Znfx1*, *ZNFX1* (previously referred to as KIAA1404 or MAD-Cap5), is specifically up-regulated in response to chemotherapeutic treatment in MCF7 and ZR-75-1 human mammary gland cell lines (Troester et al. 2004) and is also up-regulated in the serum of patients following treatment for prostate cancer (Dunphy and McNeel 2005). One conclusion drawn from these studies was that *ZNFX1* might be involved in DNA repair. If *Zfas1* indeed belongs to the same regulatory network as *Znfx1*, then we can speculate that *Zfas1* may also have some role in a DNA repair pathway.

Alignment of mouse *Zfas1* and human *ZFAS1* reveals only moderate sequence conservation, with the notable exception of the snoRNA regions conserved in three consecutive introns. This evident conservation of *Snord12*, *Snord12b*, and *Snord12c* suggests the function of these transcripts is likely to be conserved across mammals. Interestingly, despite an apparent absence of alternative splice variants of *Zfas1*, the *Zfas1*-derived snoRNAs are not present in equal proportions. The highly differential ratios of the snoRNAs suggest the degradation and/or stability of the snoRNAs can vary considerably. Determination of the half-lives of the snoRNAs confirmed this hypothesis, showing that *Snord12b* was considerably more stable than *Snord12* and *Snord12c*. Structural predictions reflected this differential stability, showing that *Snord12b*, the most highly expressed of the snoRNAs, has a structure consistent with increased stability. The differential stability/degradation of snoRNAs at the various stages of mammary development raises the hypothesis that the target region for these snoRNAs may be important during mammary gland development and, consequently, that the dysregulation of their expression levels may have important consequences in breast cancer etiology.

The moderate sequence homology of the evolutionarily conserved *Zfas1* and *ZFAS1* led us to look beyond nucleotide alignment of these orthologs. A number of ncRNAs have characteristic structures that are functional and hence are well conserved over evolutionary timescales. Most of the "classical" ncRNAs, including rRNAs, tRNAs, small nuclear RNAs (snRNAs), snoRNAs, as well as the RNA components of RNAse P and the signal recognition particle, show this evolutionary conservation of structure and function (Washietl et al. 2005). Comparison of the predicted secondary structures of the human and mouse forms of *Zfas1* revealed several distinct regions that had almost identical structures, despite sharing minimal sequence identity over these areas. The remarkable stability of *Zfas1* (half-life of >16 h), as well as the presence of conserved structures within *Zfas1*, implies that the RNA has functions beyond its role as a host for generating snoRNAs. This notion is supported by the observed lack of effect on snoRNA transcript levels upon siRNA-mediated *Zfas1* knockdown. Thus, the phenotypic effects caused by the

reduction of *Znxf1-as* indicate that, in this case, the snoRNA host transcript is itself functional. This may also be the case for many other noncoding host transcripts, as has been recently shown for the *Gas5* SNORD host gene (Kino et al. 2010), as well as host transcripts for miRNA host genes, such as H19 (Gabory et al. 2010) and BIC (Eis et al. 2005).

In summary, we show that the mature spliced transcript of an RNA that harbors C/D-box snoRNAs can function independently of the snoRNAs. This RNA is highly regulated in the developing mouse mammary gland, acts as a repressor of proliferation and differentiation, and is dysregulated in human breast cancer. Our results highlight the importance of the largely unexplored population of non-protein-coding genes in understanding the molecular basis of disease and as sources of potential biomarkers and therapeutic targets.

MATERIALS AND METHODS

Animals and mammary epithelial cells isolation

All experiments were performed with Balb/c mice, which were maintained and handled according to Australian guidelines for animal safety. All experiments were approved by the Animal Research Ethics Committee of the University of Queensland. The mice were mated and then sacrificed at day 15 of pregnancy, day 7 of lactation, and day 2 of involution. Nine mice from each stage were sacrificed, and mammary glands were dissected. One thoracic gland from each mouse was fixed for in situ hybridization and remaining glands were pooled to create three pools for each developmental stage and processed for epithelial cell purification as described previously (Tan-Wong et al. 2008). For the adult mouse tissue expression analysis, brain, liver, lung, kidney, spleen, and testis were dissected from a single male mouse, the whole mammary gland tissue was derived from a virgin female mouse, and whole embryos were harvested from a single mouse 10.5 d post-coitum.

RNA extraction

Total cellular RNA from mammary gland epithelial cells or cultured cells or other tissues from mouse was purified using Trizol (Invitrogen) according to the manufacturer's instructions. For further detail on RNA extraction and qPCR analyses, see Supplemental Methods.

Microarray analyses

Custom-designed microarrays (ArrayExpress accession number A-MEXP-1958) were synthesized by NimbleGen, and experiments performed according to the manufacturer's instructions. The noncoding transcripts targeted by the custom microarray were identified using the CRITICA software, which uses a combination of statistical and comparative parameters, such as open reading frame (ORF) length, synonymous versus nonsynonymous base substitution rates, and similarity to known proteins (Badger and Olsen 1999; Frith et al. 2006). Although we cannot eliminate the

possibility that small proteins or peptides are encoded by these transcripts (Dinger et al. 2008b), BLASTP searches of predicted ORFs indicated they did not contain any known protein motif and were not conserved in other species. Raw and normalized micro-array data is available at the ArrayExpress Data Warehouse (EMBL-EBI; ArrayExpress Accession Number E-TABM-1106). For expression analyses, see Supplemental Methods.

In situ hybridization

In situ hybridization (ISH) was performed using digoxigenin (DIG)-labeled complementary RNA probes. In vitro transcription was performed according to the manufacturer's instructions using the Promega T7/SP6 reverse transcription kit to produce sense (control) and antisense ISH probes. Section ISH was performed on 5-mm sections of paraformaldehyde-paraffin-embedded 15-d pregnant mouse mammary glands (see Supplemental Methods for details).

Northern blot analysis

Northern blot analysis was performed as previously described (Amaral et al. 2009). The *Zfas1* probe used for Northern blot analysis was the same antisense *Zfas1* PCR product that was used for in situ hybridization. Both the *Zfas1* and *Znfx1* probe (see Supplemental Table S3 for primer sequences) were random-labeled (GE Healthcare) according to the manufacturer's instructions. The snoRNA probes were prepared by amplifying the respective genes using the primers listed in Supplemental Table S3 and were randomly labeled as above.

Cell lines

Mouse HC11 cells were cultured and induced to differentiation in an eight-day assay as previously described (Naylor et al. 2005). T47D, BT474, MCF7, and N2A were cultured as described previously (Soule et al. 1973; Keydar et al. 1979; Lasfargues et al. 1979; Georgopoulou et al. 2006).

RNA stability assay

N2A cells were grown to ~50% confluence, before addition of 10 μg/mL actinomycin D to block RNA polymerase activity. RNA was extracted using RNeasy kits (Qiagen) from three biological replicates at 0, 0.5, 2, 4, 8, and 16 h after treatment. For *Znfx1* and *Zfas1*, qPCR using random hexamers was used to quantify expression relative to *GAPDH*. *Snord12*, *Snord12b*, and *Snord12c* levels were determined from RNA isolated from 0, 2, 4, 8, and 16 h after treatment and quantified as described in Supplemental Methods. The control time point (t = 0) expression level was set to 100% and treated samples shown as a percentage of the control. A one-phase exponential decay curve and half-life value were calculated using nonlinear regression with a least squares fit by Prism 5 (plateau = unconstrained, k > 0). Where no decay was present, a linear line was calculated using nonlinear regression with a least squares fit.

RNA interference

Four pairs of siRNAs (see Supplemental Table S3) designed to knockdown *Zfas1* expression and one pair of scrambled siRNAs

were purchased from Sigma. Equal quantities of HC11 cells (5×10^5) were seeded per well in 12-well plates, and the siRNA knockdown was performed as described previously (Naylor et al. 2005). Three replicates per time point were performed for both the *Znfx1/Zfas1* expression analysis (Fig. 3A) and β-casein expression assay (Fig. 3E), and quantitative PCR was performed as described above.

Proliferation assay

Quantification of cell proliferation based on the measurement of BrdU incorporation during DNA synthesis was performed on cells transfected with *Zfas1* versus those transfected with scrambled siRNA using the cell proliferation ELISA, BrdU colorimetric immunoassay kit (Roche). Twenty-four hours after siRNA transfection, cells were trypsinized, and six replicates of 12×10^3 cells were seeded per well in a 96-well plate, with the no-cells well used as a blank. Twenty-four hours after the cells were seeded in 96-well plates, the cell proliferation assay was performed according to the manufacturer's instructions.

MTT assay

Twenty-four hours after HC11 transfection with *Zfas1* versus scrambled siRNA, cells were trypsinized, and six replicates of 12×10^3 cells were seeded per well in 96-well plates, with no-cells wells used as blank. Proliferation was measured by an MTT (tetrazolium blue) conversion test and tritiated thymidine uptake (Sigma Aldrich). Briefly, 20 μL MTT (5 mg/mL) was added to each well and the cells grown at 37°C for 4 h. After addition of 100 μL of solubilization solution (10% SDS in 0.01 M HCl) cells were incubated at 37°C for a further 3 h. Specific optical density of all wells was then measured at 540 nm.

Dome formation assay

Twenty-four hours after HC11 transfection with scrambled versus *Zfas1* siRNA, cells were seeded in six-well plates. Assays for dome formation were performed as documented previously (Naylor et al. 2005). Briefly, cell differentiation was induced by the addition of o-prolactin and dexamethasone. The number of domes in each well was counted. Results presented here are from three experiments with each individual assay performed in triplicate.

Statistical analyses

Two-tailed *t*-tests were performed for qPCR, proliferation, and dome formation assays. Standard error of the mean was calculated using Prism 5.0 (GraphPad Software, Inc.). Differential microarray expression analysis was performed by the LIMMA package using Bayesian statistics (B-statistics; posterior log odds) and Benjamini-Hochberg multiple testing adjustment (see Supplemental Methods).

SUPPLEMENTAL MATERIAL

Supplemental material is available for this article.

COMPETING INTERESTS

A provisional patent for the use of *ZFAS1* as a biomarker, therapeutic, and/or a therapeutic target has been filed.

REFERENCES

Al-Shahrour F, Minguez P, Tárraga J, Montaner D, Alloza E, Vaquerizas JM, Conde L, Blaschke C, Vera J, Dopazo J. 2006. BABELOMICS: a systems biology perspective in the functional annotation of genome-scale experiments. *Nucleic Acids Res* **34:** W472–W476.

Amaral PP, Mattick JS. 2008. Noncoding RNA in development. *Mamm Genome* **19:** 454–492.

Amaral PP, Neyt C, Wilkins SJ, Askarian-Amiri ME, Sunkin SM, Perkins AC, Mattick JS. 2009. Complex architecture and regulated expression of the Sox2ot locus during vertebrate development. *RNA* **15:** 2013–2027.

Amaral PP, Clark MB, Gascoigne DK, Dinger ME, Mattick JS. 2010. lncRNAdb: a reference database for long noncoding RNAs. *Nucleic Acids Res* **39:** D146–D151.

Babak T, Blencowe BJ, Hughes TR. 2005. A systematic search for new mammalian noncoding RNAs indicates little conserved intergenic transcription. *BMC Genomics* **6:** 104. doi: 10.1186/1471-2164-6-104.

Badger JH, Olsen GJ. 1999. CRITICA: Coding region identification tool invoking comparative analysis. *Mol Biol Evol* **16:** 512–524.

Bejerano G, Pheasant M, Makunin I, Stephen S, Kent WJ, Mattick JS, Haussler D. 2004. Ultraconserved elements in the human genome. *Science* **304:** 1321–1325.

Birney E, Stamatoyannopoulos JA, Dutta A, Guigo R, Gingeras TR, Margulies EH, Weng Z, Snyder M, Dermitzakis ET, Thurman RE, et al. 2007. Identification and analysis of functional elements in 1% of the human genome by the ENCODE pilot project. *Nature* **447:** 799–816.

Brosius J. 2005. Waste not, want not–transcript excess in multicellular eukaryotes. *Trends Genet* **21:** 287–288.

Calin GA, Liu CG, Ferracin M, Hyslop T, Spizzo R, Sevignani C, Fabbri M, Cimmino A, Lee EJ, Wojcik SE, et al. 2007. Ultra-conserved regions encoding ncRNAs are altered in human leukemias and carcinomas. *Cancer Cell* **12:** 215–229.

Carninci P, Kasukawa T, Katayama S, Gough J, Frith MC, Maeda N, Oyama R, Ravasi T, Lenhard B, Wells C, et al. 2005. The transcriptional landscape of the mammalian genome. *Science* **309:** 1559–1563.

Dieci G, Preti M, Montanini B. 2009. Eukaryotic snoRNAs: A paradigm for gene expression flexibility. *Genomics* **94:** 83–88.

Dinger ME, Amaral PP, Mercer TR, Pang KC, Bruce SJ, Gardiner BB, Askarian-Amiri ME, Ru K, Solda G, Simons C, et al. 2008a. Long noncoding RNAs in mouse embryonic stem cell pluripotency and differentiation. *Genome Res* **18:** 1433–1445.

Dinger ME, Pang KC, Mercer TR, Mattick JS. 2008b. Differentiating protein-coding and noncoding RNA: Challenges and ambiguities. *PLoS Comput Biol* **4:** e1000176. doi: 10.1371/journal.pcbi.1000176.

Dinger ME, Amaral PP, Mercer TR, Mattick JS. 2009. Pervasive transcription of the eukaryotic genome: Functional indices and conceptual implications. *Brief Funct Genomics Proteomics* **8:** 407–423.

Dong XY, Guo P, Boyd J, Sun X, Li Q, Zhou W, Dong JT. 2009. Implication of snoRNA U50 in human breast cancer. *J Genet Genomics* **36:** 447–454.

Dunphy EJ, McNeel DG. 2005. Antigen-specific IgG elicited in subjects with prostate cancer treated with flt3 ligand. *J Immunother* **28:** 268–275.

Eis PS, Tam W, Sun L, Chadburn A, Li Z, Gomez MF, Lund E, Dahlberg JE. 2005. Accumulation of miR-155 and BIC RNA in human B cell lymphomas. *Proc Natl Acad Sci* **102:** 3627–3632.

Ender C, Krek A, Friedlander MR, Beitzinger M, Weinmann L, Chen W, Pfeffer S, Rajewsky N, Meister G. 2008. A human snoRNA with microRNA-like functions. *Mol Cell* **32:** 519–528.

Engstrom PG, Suzuki H, Ninomiya N, Akalin A, Sessa L, Lavorgna G, Brozzi A, Luzi L, Tan SL, Yang L, et al. 2006. Complex loci in human and mouse genomes. *PLoS Genet* **2:** e47. doi: 10.1371/journal.pgen.0020047.

Feng J, Bi C, Clark BS, Mady R, Shah P, Kohtz JD. 2006. The Evf-2 noncoding RNA is transcribed from the Dlx-5/6 ultraconserved region and functions as a Dlx-2 transcriptional coactivator. *Genes Dev* **20:** 1470–1484.

Frith MC, Bailey TL, Kasukawa T, Mignone F, Kummerfeld SK, Madera M, Sunkara S, Furuno M, Bult CJ, Quackenbush J, et al. 2006. Discrimination of non-protein-coding transcripts from protein-coding mRNA. *RNA Biol* **3:** 40–48.

Gabory A, Jammes H, Dandolo L. 2010. The H19 locus: Role of an imprinted non-coding RNA in growth and development. *Bioessays* **32:** 473–480.

Georgopoulou N, Hurel C, Politis PK, Gaitanou M, Matsas R, Thomaidou D. 2006. BM88 is a dual function molecule inducing cell cycle exit and neuronal differentiation of neuroblastoma cells via cyclin D1 down-regulation and retinoblastoma protein hypophosphorylation. *J Biol Chem* **281:** 33606–33620.

Guttman M, Amit I, Garber M, French C, Lin MF, Feldser D, Huarte M, Zuk O, Carey BW, Cassady JP, et al. 2009. Chromatin signature reveals over a thousand highly conserved large non-coding RNAs in mammals. *Nature* **458:** 223–227.

Hennighausen L, Robinson GW. 1998. Think globally, act locally: The making of a mouse mammary gland. *Genes Dev* **12:** 449–455.

Hennighausen L, Robinson GW. 2001. Signaling pathways in mammary gland development. *Dev Cell* **1:** 467–475.

Hernandez A, Garcia B, Obregon MJ. 2007. Gene expression from the imprinted Dio3 locus is associated with cell proliferation of cultured brown adipocytes. *Endocrinology* **148:** 3968–3976.

Huang ZP, Zhou H, He HL, Chen CL, Liang D, Qu LH. 2005. Genome-wide analyses of two families of snoRNA genes from *Drosophila melanogaster*, demonstrating the extensive utilization of introns for coding of snoRNAs. *RNA* **11:** 1303–1316.

Huarte M, Rinn JL. 2010. Large non-coding RNAs: Missing links in cancer? *Hum Mol Genet* **19:** R152–R161.

Huttenhofer A, Kiefmann M, Meier-Ewert S, O'Brien J, Lehrach H, Bachellerie JP, Brosius J. 2001. RNomics: An experimental approach that identifies 201 candidates for novel, small, non-messenger RNAs in mouse. *EMBO J* **20:** 2943–2953.

Kapranov P, Cawley SE, Drenkow J, Bekiranov S, Strausberg RL, Fodor SP, Gingeras TR. 2002. Large-scale transcriptional activity in chromosomes 21 and 22. *Science* **296:** 916–919.

Kapranov P, Cheng J, Dike S, Nix DA, Duttagupta R, Willingham AT, Stadler PF, Hertel J, Hackermuller J, Hofacker IL, et al. 2007a. RNA maps reveal new RNA classes and a possible function for pervasive transcription. *Science* **316:** 1484–1488.

Kapranov P, Willingham AT, Gingeras TR. 2007b. Genome-wide transcription and the implications for genomic organization. *Nat Rev Genet* **8:** 413–423.

Keydar I, Chen L, Karby S, Weiss FR, Delarea J, Radu M, Chaitcik S, Brenner HJ. 1979. Establishment and characterization of a cell line of human breast carcinoma origin. *Eur J Cancer* **15:** 659–670.

Kino T, Hurt DE, Ichijo T, Nader N, Chrousos GP. 2010. Noncoding RNA gas5 is a growth arrest- and starvation-associated repressor of the glucocorticoid receptor. *Sci Signal* **3:** ra8. doi: 10.11126/scisignal.2000568.

Lasfargues EY, Coutinho WG, Dion AS. 1979. A human breast tumor cell line (BT-474) that supports mouse mammary tumor virus replication. *In Vitro* **15:** 723–729.

Master SR, Hartman JL, D'Cruz CM, Moody SE, Keiper EA, Ha SI, Cox JD, Belka GK, Chodosh LA. 2002. Functional microarray analysis of mammary organogenesis reveals a developmental role in adaptive thermogenesis. *Mol Endocrinol* **16:** 1185–1203.

Mazar J, Sinha S, Dinger ME, Mattick JS, Perera RJ. 2010. Protein-coding and non-coding gene expression analysis in differentiating human keratinocytes using a three-dimensional epidermal equivalent. *Mol Genet Genomics* **284:** 1–9.

Mercer TR, Dinger ME, Sunkin SM, Mehler MF, Mattick JS. 2008. Specific expression of long noncoding RNAs in the mouse brain. *Proc Natl Acad Sci* **105:** 716–721.

Mercer TR, Dinger ME, Mattick JS. 2009. Long noncoding RNAs: Insights into function. *Nat Rev Genet* **10:** 155–159.

Mercer TR, Qureshi IA, Gokhan S, Dinger ME, Li G, Mattick JS, Mehler MF. 2010. Long noncoding RNAs in neuronal-glial fate specification and oligodendrocyte lineage maturation. *BMC Neurosci* **11:** 14. doi: 10.1186/1471-2202-11-14.

Metcalfe AD, Gilmore A, Klinowska T, Oliver J, Valentijn AJ, Brown R, Ross A, MacGregor G, Hickman JA, Streuli CH. 1999. Developmental regulation of Bcl-2 family protein expression in the involuting mammary gland. *J Cell Sci* **112:** 1771–1783.

Mosmann T. 1983. Rapid colorimetric assay for cellular growth and survival: Application to proliferation and cytotoxicity assays. *J Immunol Methods* **65:** 55–63.

Mourtada-Maarabouni M, Pickard MR, Hedge VL, Farzaneh F, Williams GT. 2009. GAS5, a non-protein-coding RNA, controls apoptosis and is down-regulated in breast cancer. *Oncogene* **28:** 195–208.

Naylor MJ, Oakes SR, Gardiner-Garden M, Harris J, Blazek K, Ho TW, Li FC, Wynick D, Walker AM, Ormandy CJ. 2005. Transcriptional changes underlying the secretory activation phase of mammary gland development. *Mol Endocrinol* **19:** 1868–1883.

Pang KC, Dinger ME, Mercer TR, Malquori L, Grimmond SM, Chen W, Mattick JS. 2009. Genome-wide identification of long non-coding RNAs in CD8+ T cells. *J Immunol* **182:** 7738–7748.

Pelczar P, Filipowicz W. 1998. The host gene for intronic U17 small nucleolar RNAs in mammals has no protein-coding potential and is a member of the 5′-terminal oligopyrimidine gene family. *Mol Cell Biol* **18:** 4509–4518.

Ponjavic J, Ponting CP, Lunter G. 2007. Functionality or transcriptional noise? Evidence for selection within long noncoding RNAs. *Genome Res* **17:** 556–565.

Ravasi T, Suzuki H, Pang KC, Katayama S, Furuno M, Okunishi R, Fukuda S, Ru K, Frith MC, Gongora MM, et al. 2006. Experimental validation of the regulated expression of large numbers of non-coding RNAs from the mouse genome. *Genome Res* **16:** 11–19.

Robinson GW, McKnight RA, Smith GH, Hennighausen L. 1995. Mammary epithelial cells undergo secretory differentiation in cycling virgins but require pregnancy for the establishment of terminal differentiation. *Development* **121:** 2079–2090.

Song Z, Krishna S, Thanos D, Strominger JL, Ono SJ. 1994. A novel cysteine-rich sequence-specific DNA-binding protein interacts with the conserved X-box motif of the human major histocompatibility complex class II genes via a repeated Cys-His domain and functions as a transcriptional repressor. *J Exp Med* **180:** 1763–1774.

Soule HD, Vazquez J, Long A, Albert S, Brennan M. 1973. A human cell line from a pleural effusion derived from a breast carcinoma. *J Natl Cancer Inst* **51:** 1409–1416.

Struhl K. 2007. Transcriptional noise and the fidelity of initiation by RNA polymerase II. *Nat Struct Mol Biol* **14:** 103–105.

Sunwoo H, Dinger ME, Wilusz JE, Amaral PP, Mattick JS, Spector DL. 2009. MEN varepsilon/beta nuclear-retained non-coding RNAs are up-regulated upon muscle differentiation and are essential components of paraspeckles. *Genome Res* **19:** 347–359.

Taft RJ, Glazov EA, Lassmann T, Hayashizaki Y, Carninci P, Mattick JS. 2009. Small RNAs derived from snoRNAs. *RNA* **15:** 1233–1240.

Tan-Wong SM, French JD, Proudfoot NJ, Brown MA. 2008. Dynamic interactions between the promoter and terminator regions of the mammalian BRCA1 gene. *Proc Natl Acad Sci* **105:** 5160–5165.

Trinklein ND, Aldred SF, Hartman SJ, Schroeder DI, Otillar RP, Myers RM. 2004. An abundance of bidirectional promoters in the human genome. *Genome Res* **14:** 62–66.

Troester MA, Hoadley KA, Sorlie T, Herbert BS, Borresen-Dale AL, Lonning PE, Shay JW, Kaufmann WK, Perou CM. 2004. Cell-type-specific responses to chemotherapeutics in breast cancer. *Cancer Res* **64:** 4218–4226.

Vizcaino JA, Cote R, Reisinger F, Foster JM, Mueller M, Rameseder J, Hermjakob H, Martens L. 2009. A guide to the Proteomics Identifications Database proteomics data repository. *Proteomics* **9:** 4276–4283.

Wang H, Iacoangeli A, Lin D, Williams K, Denman RB, Hellen CU, Tiedge H. 2005. Dendritic BC1 RNA in translational control mechanisms. *J Cell Biol* **171:** 811–821.

Wang Z, Zang C, Rosenfeld JA, Schones DE, Barski A, Cuddapah S, Cui K, Roh TY, Peng W, Zhang MQ, et al. 2008. Combinatorial patterns of histone acetylations and methylations in the human genome. *Nat Genet* **40:** 897–903.

Washietl S, Hofacker IL, Lukasser M, Huttenhofer A, Stadler PF. 2005. Mapping of conserved RNA secondary structures predicts thousands of functional noncoding RNAs in the human genome. *Nat Biotechnol* **23:** 1383–1390.

Wilusz JE, Sunwoo H, Spector DL. 2009. Long noncoding RNAs: Functional surprises from the RNA world. *Genes Dev* **23:** 1494–1504.

Yan MD, Hong CC, Lai GM, Cheng AL, Lin YW, Chuang SE. 2005. Identification and characterization of a novel gene Saf transcribed from the opposite strand of Fas. *Hum Mol Genet* **14:** 1465–1474.

Yang JH, Zhang XC, Huang ZP, Zhou H, Huang MB, Zhang S, Chen YQ, Qu LH. 2006. snoSeeker: An advanced computational package for screening of guide and orphan snoRNA genes in the human genome. *Nucleic Acids Res* **34:** 5112–5123.

Zucchi I, Bini L, Albani D, Valaperta R, Liberatori S, Raggiaschi R, Montagna C, Susani L, Barbieri O, Pallini V, et al. 2002. Dome formation in cell cultures as expression of an early stage of lactogenic differentiation of the mammary gland. *Proc Natl Acad Sci* **99:** 8660–8665.